

Influence of Fe₃O₄ and CTABr on the Rate of Degradation of Methylene Blue by H₂O₂

Mohd Shaban Ansari¹, Kashif Raees¹, Elham S. Aazam², M. Z. A. Rafiquee^{1,*}

¹Department of Applied Chemistry, Z.H. College of Engineering and Technology, Aligarh Muslim University, Aligarh 202002, India

²Department of Chemistry, King Abdul Aziz University, Jeddah, Saudi Arabia

*Corresponding author: E-mail: drrafiquee@gmail.com

DOI: 10.5185/amlett.2021.021602

The kinetics of the oxidation of methylene blue (MB) by H₂O₂ in the presence of iron oxide nanoparticles has been studied. The nanoparticles of iron oxide (Fe₃O₄) were synthesized and characterized physico-chemical techniques. The XRD studies showed its crystalline nature. The VSM study was carried out to determine the values of the magnetic saturation parameter ~ 40.00 emu/g. The particles were of spherical shape with particle size distribution centered at 12 ± 2 nm. The FT-IR spectra indicated the presence of peaks at 585 cm⁻¹ and 459 cm⁻¹ due to Fe-O bond vibrations. The peak at 3424 cm⁻¹ was assigned to the O-H stretching vibration. The H-O-H bending appeared at 1631 cm⁻¹. The Fe₃O₄ nanoparticles enhanced the rate of degradation of MB. The oxidation rate increased with the increase in Fe₃O₄. At pH 3, the maximum rate of oxidation of MB was observed. The rate of reaction increased with the increase in [H₂O₂] in the absence of Fe₃O₄. But in the presence of Fe₃O₄, the rate constant *versus* [H₂O₂] showed peaked behaviour. The CTABr increased the rate of oxidation of MB by H₂O₂ in the presence of Fe₃O₄ nanoparticles.

Introduction

Dyes are widely used in textiles industries during dyeing and printing processes and the excess amount of dyes are released into the effluent streams as waste after colouring the cloth [1]. The release of coloured waste water involving dyes, from textiles and other industries pollute the water and make it undesirable and may cause serious environmental problems [2]. These pollutants are oncogenic and mutagenic and produce the possible risk of bioaccumulation [3]. The wastewater containing dyes prevent light transmission and causes harm to both flora and fauna, and may cause eco-toxic hazard to human and aquatic life [4]. Methylene Blue chemically is commonly known as methylthioninium chloride is a heterocyclic aromatic chemical compound with molecular formula C₁₆H₁₈ClN₃S. MB is a cationic dye widely used in industries such as textiles, plastics, paper, cotton, silk, leather, food and cosmetics to colour products [5]. MB is a synthetic dye and is highly soluble, stable and has biotoxicity in water and thus can threaten the ecological balance even the survival of human being owing to their toxicity, carcinogenicity, and bioaccumulation [6]. MB can cause eye irritation in humans as well as in animals, allergy and cancer due to its toxicity [7]. If ingested the water containing MB, it will cause nausea, hard breathing, vomiting, methemoglobinemia, mental disorder and sweating [8,9]. Thus, it is necessary to develop new and cost-effective technologies to remove MB from wastewater.

The removal of dyes from wastewater is a primary concern for the environmentalists. Many methods are

available for the removal of dyes from water such as reverse osmosis, ion exchange method, precipitation, adsorption, ozone treatment, catalytic reduction, biodegradation, ultrasonic decomposition, coagulation, electro-coagulation, chemical oxidation and nano-filtration etc. [10-13]. Extensive studies are available on the removal of methylene blue (MB) through the applications of low-cost adsorbents from waters. The adsorption techniques are usually useful for the removal of non-biodegradable wastes but its disposal may raise the subsequent environmental issues [14-16]. The other factors that contribute towards the drawbacks of these techniques are high cost, long processing time, high energy consumption, regeneration difficulty, and simple transfer of pollutants from one phase to another [17,18]. Oxidation by the Fenton's reagent is one of the most effective methods for destroying the organic wastes. It consists of a mixture of hydrogen peroxide and iron (II) ion (H₂O₂ + Fe²⁺). It plays an important role in free radical biology, medicine, environmental systems, and environment protection engineering including the wastewater treatment and remediation of groundwater.

Recently magnetic nanoparticles (MNPs), especially Fe₃O₄, are widely used catalyst for the removal of dyes from waste water solution since Fe₃O₄ NPs are inert, inexpensive, nontoxic, biocompatible, having super magnetic properties and can be reused and recycled with the help of simple magnets [19-21]. These special cubic spinel structure of magnetite display catalytic activity, can be useful in the removal of various dyes and organic wastes from water [22]. The Fe₃O₄ NPs act as Fenton-like catalyst for the degradation of MB through generating hydroxyl

radical which attack the dye and degrade it [23-25]. The dyes are usually oxidized into smaller fractions which are biodegradable and harmless products [26]. The present work has been undertaken with the aim to synthesize magnetic nanoparticles (Fe_3O_4) and to use them as a low-cost catalyst. The method will be effective in converting the dye MB into non-toxic harmless material. The small amount of nanoparticle can oxidize large amount of dye effectively and efficiently. In pursue of these objectives the kinetics experiments have been adopted to obtain the optimum reaction condition for the effective removal of MB from the waste water. The influence of the variation in the amount of iron nanoparticles, $[\text{H}_2\text{O}_2]$, pH, temperature, *etc.* on the rate of degradation of MB was investigated. The effect of cationic surfactant, cetyltrimethyl ammonium bromide (CTABr) on the rate of degradation of MB was also studied and the observed results are discussed herewith.

Experimental

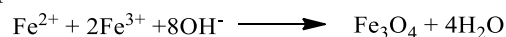
Materials

Methylene blue (MB), HCl (36%) and H_2O_2 (35% w/v) were purchased from (Merck, Mumbai, India). CTABr (99%, CDH, New Delhi), Ferric Chloride (97.0%; CDH, New Delhi, India), Ferrous Chloride dihydrate (99%; CDH, New Delhi), Sodium hydroxide pellets (97%, Merck, Mumbai, India), Liquor ammonia (25% with a purity index of 99%, Thermo Fisher Scientific, Mumbai, India) were purchased and were used as supplied. The remaining materials were reagent grades. Doubly distilled water was used to prepare the stock solutions. The strength of the stock solution of sodium hydroxide and surfactant (CTABr) were 1.0 mol dm^{-3} and $1.0 \times 10^{-2} \text{ mol dm}^{-3}$, respectively. The required amount (4.0 g) of NaOH was dissolved in 100 mL distilled water in a standard flask and then standardized with oxalic acid solution. 3.64 g of CTABr was dissolve in 100 mL double distilled water. 100.0 ppm solution of MB was prepared in 100 mL standard flask by dissolving in double distilled water. 25 mL of hydrogen peroxide (H_2O_2) was diluted to 250 mL and then the solution was standardized. 0.1 M stock solution of HCl was prepared in 100 mL distilled water.

Synthesis of Fe_3O_4 Magnetic Nanoparticles (MNPs) by Co-precipitation Method

MNPs were synthesized by adopting the procedures and methods described earlier [27-29]. The co-precipitation method was adopted to synthesize the nanoparticles. 20.0 g of FeCl_3 (0.4M) and 10.0 g of $\text{FeCl}_2 \cdot 2\text{H}_2\text{O}$ (0.2M) were dissolved in approximately 300 mL double distilled taken into a 1000 mL conical flask. The N_2 gas bubbled continuously to remove dissolved gases. The solution was stirred and 200 mL of 25% ammonium hydroxide was added to it. The pH of the solution was further raised by adding 2.0 M of NaOH solution. The temperature of the mixture was increased to about 70°C with constant bubbling of N_2 gas. The fine particles precipitated was

filtered and washed with acetone /double distilled water. The precipitate was then left at 70°C for ~5 hours. The following reaction summarizes the formation of iron oxide nanoparticles:



Kinetic experiments

The kinetic experiments were performed spectrophotometrically using a GENESYS 10S UV/Visible spectrophotometer (Thermo Fisher Scientific, Medison, USA). The instrument was provided with multiple cell holders in which a 3.0 mL capacity quartz cuvette with path length of 10 mm was used to measure the absorbance. All the kinetic experiments were performed at a constant temperature of $25.0 \pm 0.2^\circ\text{C}$ or at the desired temperature stated. The solutions of the dye and MNPs were taken into round bottom three necked flask of 100 mL capacity kept in a thermostated water-bath. The reaction was started with the addition of H_2O_2 to the dye (MB) solution containing required amount of MNPs. The pH of the solution was maintained constant using HCl or NaOH solution. The concentration of the dye was determined at constant interval by measuring the absorbance at 665 nm. The concentration of H_2O_2 was kept in excess over [MB] during all these kinetic experiments. The pseudo-first-order rate constant values were obtained from the slopes of the plots of $\ln(\text{absorbance})$ versus time. Each kinetic run was carried out in triplicate and the observed value of rate constant was obtained within 5% error limits.

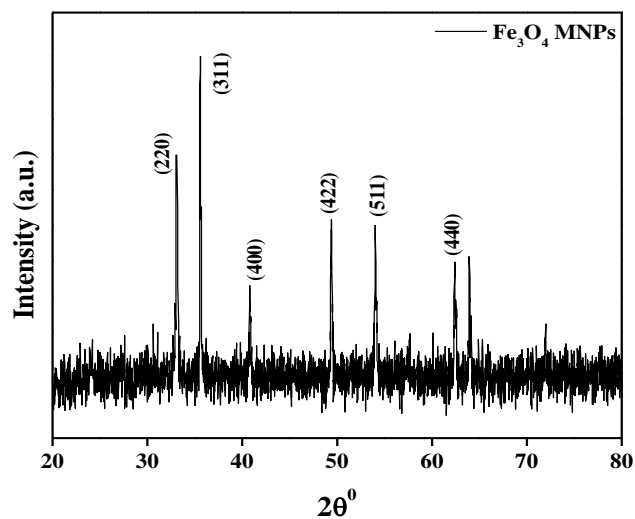


Fig. 1. X-ray diffraction patterns obtained for the synthesized Fe_3O_4 .

Results and discussion

Characterization of Magnetic Nanoparticles (MNPs)

The MNPs were characterized by X-ray diffraction method (using X-ray diffractometer, MiniFlex II, Rigaku, Japan) equipped with a Cu $\text{K}\alpha$ radiation source (with $\lambda = 1.5406 \text{ nm}$). The XRD patterns (Fig. 1) obtained confirmed the crystalline nature of the synthesized nanoparticles with planes (220), (311), (400), (422), (511) and (440) [30].

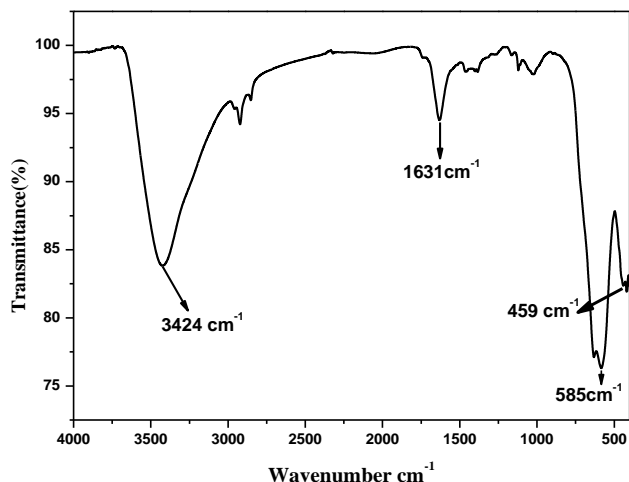


Fig. 2. FTIR spectra of Fe₃O₄.

The MNPs were further characterized by Nicolet iS50 FT-IR Spectrometer (Thermo Fisher Scientific, Madison, USA). The FT-IR spectra of pure Fe₃O₄ MNPs are shown in Fig. 2. The two peaks appearing at 585cm⁻¹ and 459cm⁻¹ correspond to the Fe-O bond vibrations in Fe₃O₄ arising due to difference in bond length and confirm the spinal structure of Fe₃O₄ nanoparticles [31]. The peak at 3424 cm⁻¹ is due to the O-H stretching vibration arising from the hydroxyl group is likely due to the presence of water molecules associated with Fe₃O₄ [32]. The H-O-H bending of water molecule is also located at 1631 cm⁻¹ in Fe₃O₄ nanoparticles [33]. Field Emission Scanning Electron Microscope (FESEM, JSM-7800F, JEOL, Japan) and Transmission Electron Microscope (HRTEM, Techno, FEI) were used to determine the morphology, shape and size of the nanoparticles. The SEM micrograph of the synthesized magnetite nanoparticles Fe₃O₄ is shown in Fig. 3(a). It can be observed that the nanoparticles exhibit spherical surface morphology with the agglomeration of many ultrafine particles. These particles have the size range from lower than 100 nm to 1µm scale with low polydispersity. Corresponding to the TEM micrograph presented in Fig. 3(b), the pristine Fe₃O₄ NPs have spherical shape with a narrow particle size distribution centered at 12 ± 2 nm and are shown in the histogram (Fig. 3(b)). The magnetic behavior of Fe₃O₄ NPs has been studied by using Vibrating Sample Magnetometer (VSM Lake Shore-7404). The value of specific magnetic saturation parameter for Fe₃O₄ nanoparticles was observed at 40.00 emu/g as shown in Fig. 4.

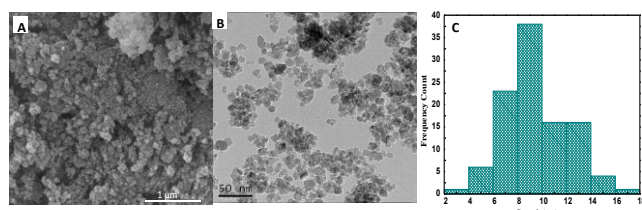


Fig. 3. SEM image of Fe₃O₄ (A), TEM image of Fe₃O₄ (B) and histogram showing the particle size distribution.

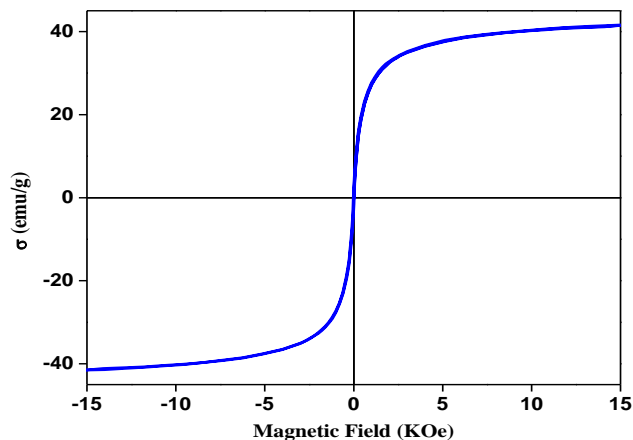
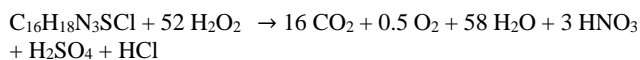


Fig. 4. Hysteresis curve for Fe₃O₄.

Degradation of methylene blue by hydrogen peroxide

The consecutive scans of the solution containing the dye MB (2.0 ppm) and H₂O₂ (2.0 × 10⁻¹ mol dm⁻³) were recorded at a constant intervals in the visible region (500-750 nm) spectrophotometrically at 25 °C. The pH of the solution was fixed at 3.0 with the help of HCl solution. The spectra presented in Fig. 5(a) display the decrease in the intensity of absorbance at λ_{max} (665 nm). The decrease in the intensities of absorbance is due to the oxidation of MB dye by the hydrogen peroxide. Fig. 5(b) is the consecutive scans of the solution containing MB (2.0 ppm), H₂O₂ (2.0 × 10⁻¹ mol dm⁻³) and 0.1% (w/v) Fe₃O₄ MNPs. The decrease in the rate of the absorbance intensity is enhanced due to the presence of iron oxide nanoparticles. The oxidation of the dye is carried out by H₂O₂. The dye is degraded into non-toxic reaction products e.g., carbon dioxide, oxygen and acids. The following overall reaction (Scheme 1) presents the oxidation of the MB dye [34].



Scheme 1

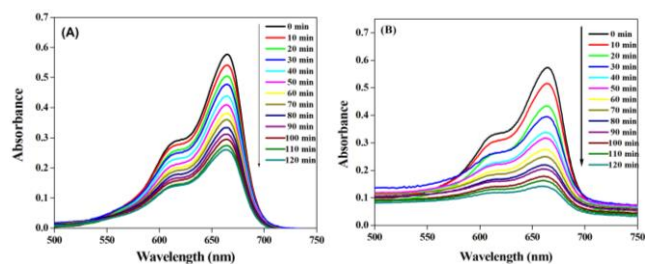
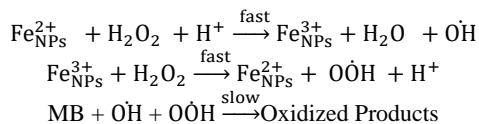


Fig. 5. Consecutive scans recorded by UV-Visible spectrophotometer for the solution containing: (A) MB (2.0 ppm) and H₂O₂ (2.0×10⁻¹ mol dm⁻³); (B) MB (2.0 ppm), H₂O₂ (2.0 × 10⁻¹ mol dm⁻³) and Fe₃O₄ (0.1% w/v) at the intervals of 10 minutes at pH 3.0 and Temperature 25 °C.

Degradation of methylene blue by hydrogen peroxide in the presence of Fe₃O₄ magnetic nanoparticles

The spectra shown in the Fig. 5(a) and Fig. 5(b), indicates that the rate of oxidation of dye is faster in the presence of 0.1% (w/v) Fe₃O₄ MNPs. The enhancement in the rate of reaction in the presence of MNPs is attributed to the

catalytic activity of Fe_3O_4 . The values of the observed initial rate constant were independent on the concentrations of MB. To investigate the influence of MNPs on the rate of the reaction, the amount of Fe_3O_4 was increased from 0.02 % to 0.2 % (w/v) keeping the concentrations of H_2O_2 and MB fixed at $2.0 \times 10^{-1} \text{ mol dm}^{-3}$ and 2 ppm, respectively. The increase in the amount of MNPs increased the rate of reaction as shown in Fig. 6. The iron oxide nanoparticles interacts with the hydrogen peroxide to generate reactive OH radicals through many different reaction pathways [35]. In case of homogeneous Fenton reactions, the oxidized Fe^{3+} has tendency to precipitate, whereas, the iron oxides nanomaterials decompose H_2O_2 via surface bound iron, avoiding precipitation of iron [36]. The generation of OH and OOH radicals from H_2O_2 at the MNPs surfaces are quite fast. The generated HO^\cdot radicals attack the benzene ring of the dye causing its degradation. The oxidation of MB by these OH and OOH radicals is considered to be slow step as presented through Scheme 2.



Scheme 2

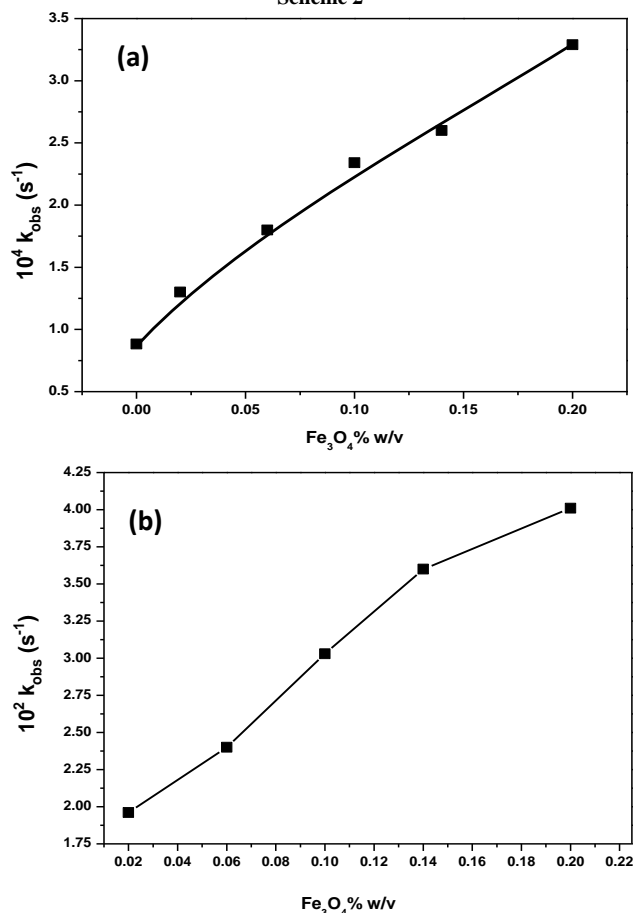


Fig. 6. Plots of k_{obs} versus $[\text{Fe}_3\text{O}_4]$ for the degradation of MB in the absence (a) and presence of CTABr (b). Reaction conditions: $[\text{MB}] = 2.0 \text{ ppm}$, $[\text{H}_2\text{O}_2] = 2.0 \times 10^{-1} \text{ mol dm}^{-3}$, $[\text{CTABr}] = 2.0 \times 10^{-2} \text{ mol dm}^{-3}$ pH=3 and Temperature = 25°C .

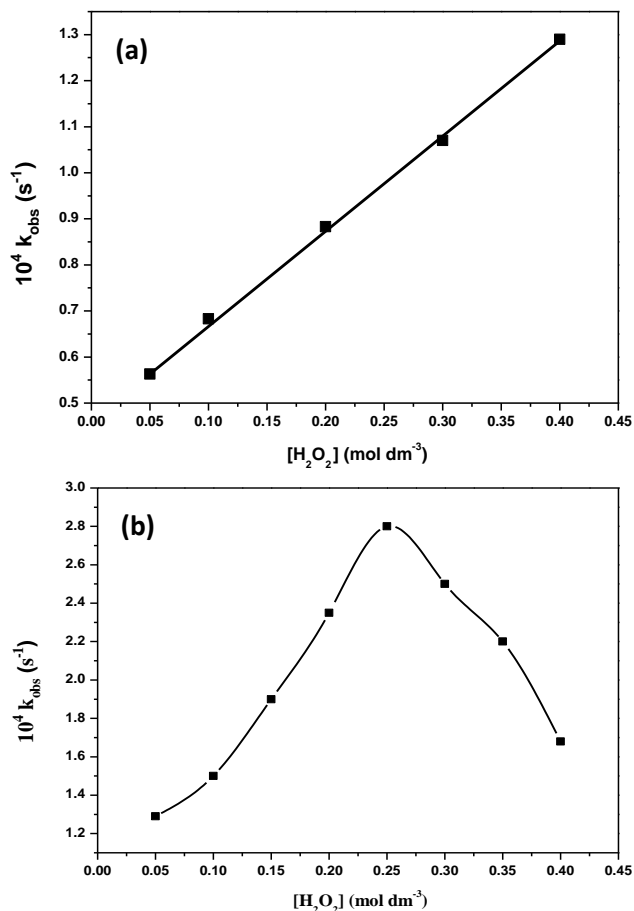
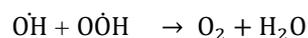
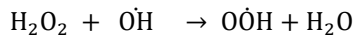


Fig. 7. Plot of k_{obs} versus $[\text{H}_2\text{O}_2]$ for degradation of MB in the absence (a) and presence of Fe_3O_4 (b). Reaction conditions: $[\text{MB}] = 2.0 \text{ ppm}$, $[\text{Fe}_3\text{O}_4] = 0.1 \text{ \% w/v}$ at pH 3.0 and Temperature 25°C .

The nanoparticles on interaction with hydrogen peroxide generates OH and OOH radicals. These radicals are highly reactive and increases the rate of oxidation of MB. It is hence observed that the increase in the amount of nanoparticles increases OH and OOH radicals and therefore the rate of oxidation of MB increases with the increase in MNPs (Fig. 6(a)). Similarly, it is observed that the values of rate constant increase with the increase in the concentration of H_2O_2 in the range from $5.0 \times 10^{-2} \text{ mol dm}^{-3}$ to $4.0 \times 10^{-1} \text{ mol dm}^{-3}$ at constant concentration of MB (2.0 ppm) (Fig. 7(a)). In the absence of Fe_3O_4 , the rate of degradation of MB increases linearly with increase in $[\text{H}_2\text{O}_2]$ whereas in the presence of Fe_3O_4 , the rate of reaction increases with the increase in $[\text{H}_2\text{O}_2]$ upto a certain concentration of H_2O_2 at fixed amount of Fe_3O_4 . On further increase in the concentration of $[\text{H}_2\text{O}_2]$, the rate of degradation of MB decreases (Fig. 7(b)), showing a peaked behaviour. The maximum value of rate constant was obtained at $2.50 \times 10^{-1} \text{ mol dm}^{-3} \text{ H}_2\text{O}_2$. Thus, the rate of reaction is decreased at lower as well as at higher concentrations of H_2O_2 . It may be due the reaction involved in the removal of the free radical through the following reactions.



Thus, at higher $[H_2O_2]$, more and more $\dot{O}H$ and $O\dot{O}H$ radicals are generated and instead of undergoing reaction with MB, they combine themselves quickly to give non-reactive oxygen gas. Additionally, at higher concentrations of H_2O_2 there is a competition between the substrate and H_2O_2 for the reaction with $\dot{O}H$ radical.



Thus, at the higher concentrations, H_2O_2 molecules act as scavenger of $\dot{O}H$ radicals to produce per hydroxyl radical, $O\dot{O}H$ which has lower activities for oxidation reactions. Hence a decrease in the values of rate constants is observed at higher $[H_2O_2]$. The plot in **Fig. 7(b)** shows the peaked behaviour of variation in the observed rate constant against $[H_2O_2]$.

The recombination of the $\dot{O}H$ radicals can also not be ruled out for the decrease in the rate of reactions at higher $[H_2O_2]$ [37,38].



Influence of pH on the degradation of methylene blue by hydrogen peroxide in the presence of Fe_3O_4 magnetic nanoparticles

The rate of degradation of the MB dye is highly pH dependent. To determine the optimum pH for the oxidation of MB in the presence of 0.1% w/v Fe_3O_4 , the kinetics experiment was carried out at different pH by taking 2.0 ppm of MB at 25 °C. The pH was changed from 1.0 to 10.0 keeping the concentration of and H_2O_2 constant at $2.0 \times 10^{-1} \text{ mol dm}^{-3}$. The observed rate constants values shown in **Fig. 8** clearly indicate that the rate of degradation of the dye is the maximum at pH 3.0. The rate constant values increased with the increase in pH up to 3, thereafter, decreased on further increasing the pH value from 3.0. At high concentration of H^+ ions (at $pH < 3.0$) peroxide get solvated to form stable oxonium ions which lowers the activity of H_2O_2 and restrict the generation of hydroxyl radical. Moreover, the excess of H^+ ions acts as hydroxyl radical scavenger [39,40]. The low activity for the degradation of MB at high pH is due to the formation of hydroxyl complexes with Fe^{3+} which blocks the active sites of iron [41]. Additionally, the hydroperoxyl anion at high pH decreases the concentration of H_2O_2 and hydroxyl radicals. Therefore, the activity of hydroxyl radicals decreases at higher pH values.

Influence of temperature on the degradation of methylene blue by hydrogen peroxide in the presence of Fe_3O_4 magnetic nanoparticles

The kinetic parameters for the degradation of MB at the Fe_3O_4 surface were calculated by carrying out the experimental work at different temperatures. The values of rate constant were obtained in the temperature range from 25°C to 60°C at pH 3.0 and keeping the fixed concentrations of dye (2.0 ppm), H_2O_2 ($2.0 \times 10^{-1} \text{ mol dm}^{-3}$) and Fe_3O_4 (0.1% w/v). The substantial increase in the rate of the oxidation of dye was observed on increasing the temperature. At temperature above 60°C, the rate of

degradation of the dye decreased because of the thermal decomposition of hydrogen peroxide at higher temperatures. The values of rate constant obtained at different temperature were used to calculate energy of activation by using Arrhenius equation (1). It gave straight line plot for $\log k$ versus $1/T$ from which the slope was determined to calculate the energy of activation.

$$\log k_{\text{obs}} = -\frac{E_a}{2.303 RT} + \log A_0 \quad (1)$$

In this equation, E_a is the activation energy (kJ/mol), R ($8.314 \text{ J mol}^{-1} \text{ K}^{-1}$) is the universal gas constant, T is the temperature in Kelvin (K), A_0 is the frequency factor and k is the measured value first-order rate constant. The activation energy has been determined from the slope and values are given in **Table 1**.

The value of ΔH (enthalpy of activation) was calculated using Eyring equation (2).

$$\ln \left(\frac{k_{\text{obs}}}{T} \right) = -\frac{\Delta H^\ddagger}{R} \frac{1}{T} + \ln \frac{k_B}{h} + \frac{\Delta S^\ddagger}{R} \quad (2)$$

Here, k_B is the Boltzmann's constant and h is the Planck's constant. A plot of $\ln(k_{\text{obs}}/T)$ versus $1/T$ produces a straight line and the values of ΔH^\ddagger and ΔS^\ddagger have been obtained from the slope and intercept, respectively. These values are given in **Table 1**.

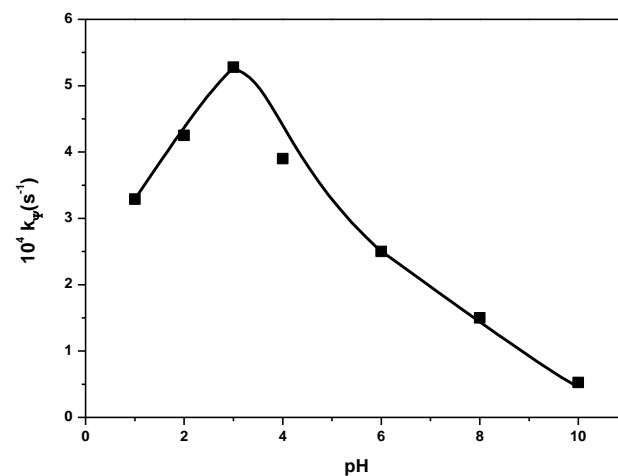


Fig. 8. Plot of k_{obs} versus pH for the degradation of MB. Reaction conditions: $[MB] = 2.0 \text{ ppm}$, $[H_2O_2] = 2.0 \times 10^{-1} \text{ mol dm}^{-3}$ and Temperature = 25 °C.

Influence of CTABr on the degradation of methylene blue by hydrogen peroxide in the presence of Fe_3O_4 magnetic nanoparticles

The rate of oxidation of MB increased on addition of the cationic surfactant (CTABr) to the solution containing Fe_3O_4 nanoparticles. The rates of degradation of MB were performed at different $[CTABr]$ varying from $5.0 \times 10^{-4} \text{ mol dm}^{-3}$ to $5.0 \times 10^{-2} \text{ mol dm}^{-3}$ at fixed concentration of Fe_3O_4 nanoparticles (0.1% w/v), H_2O_2 ($2.0 \times 10^{-1} \text{ mol dm}^{-3}$) and MB (2.0 ppm). Initially, in the concentration range from $5.0 \times 10^{-4} \text{ mol dm}^{-3}$ to $1.0 \times 10^{-2} \text{ mol dm}^{-3}$ $[CTABr]$, the rate constant values increased from $5.0 \times 10^{-3} \text{ s}^{-1}$ to

$2.5 \times 10^{-2} \text{ s}^{-1}$ (~ 5 fold), but, the further increase in the concentration of CTABr from $1.0 \times 10^{-2} \text{ mol dm}^{-3}$ to $5.0 \times 10^{-2} \text{ mol dm}^{-3}$, the increase in the rate constant values were relatively slow ($2.5 \times 10^{-3} \text{ s}^{-1}$ to $4.5 \times 10^{-2} \text{ s}^{-1}$) (Fig. 9). Owing to the surface-active tendency, it can be said that the CTABr molecules get attracted more to the surface of Fe_3O_4 nanoparticles through electrostatic attraction between the electron rich MNPs surface and positively charged CTA⁺ headgroup [42]. This results into the formation of surfactant coatings around the nanoparticles to form monolayer hemi-micelles. The hydrophobic interactions between MB and CTABr increases the local concentrations of the dye more near the Fe_3O_4 surface and results into the enhancement in the rate of reaction. At higher [CTABr], the surfactant molecules form ad-micelles *via* hydrophobic attraction between the surfactants organic tail to form layered structure around the Fe_3O_4 surface. This phenomenon blocks the active sites of Fe_3O_4 and therefore, the rate of reaction decreases at higher [CTABr]. The increase in the amount of Fe_3O_4 in the presence of CTABr increased the rate of degradation of MB by H_2O_2 (Fig. 6B).

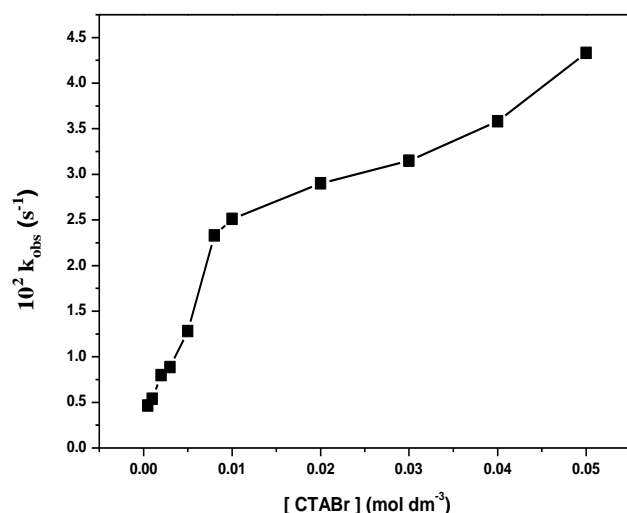


Fig. 9. Plot of k_{obs} versus [CTABr] for the degradation of MB. Reaction conditions: [MB] = 2.0 ppm, [H_2O_2] = $2.0 \times 10^{-1} \text{ mol dm}^{-3}$ and [Fe_3O_4] = 0.1 % w/v at pH 3.0 and Temperature 25 °C.

The comparative values of E_a and ΔH^\ddagger for the degradation of MB by H_2O_2 determined in the absence and presence of Fe_3O_4 and CTABr are given in Table 1. These values show the value of energy of activation (E_a) is lowest in the presence of both Fe_3O_4 and CTABr while its value is the maximum in the absence of both Fe_3O_4 and CTABr. The E_a and ΔH^\ddagger values are lower in the presence of Fe_3O_4 than H_2O_2 only. Thus, the lower energy of activation favours the reaction and accelerates the rate of reaction more in the presence of Fe_3O_4 and CTABr. The change in entropy (ΔS^\ddagger) for the formation of activated complex is negative which indicates that the transition state is more organised and orderly arranged. Thus, the activated complex formed in the presence of Fe_3O_4 presents the high degree of orderness than in the presence of CTABr.

Table 1. The values of the activation parameters for the oxidation of MB (2.0 ppm) by H_2O_2 ($2.0 \times 10^{-1} \text{ mol dm}^{-3}$) in the absence and presence of Fe_3O_4 and CTABr.

Reaction Media	E_a (kJ mol ⁻¹)	ΔH^\ddagger (kJ mol ⁻¹)	$-\Delta S^\ddagger$ (J K ⁻¹ mol ⁻¹)	R^2
H_2O_2	59.21	56.59	157.401	0.960
$\text{H}_2\text{O}_2 + \text{Fe}_3\text{O}_4$	50.66	45.15	183.714	0.965
$\text{H}_2\text{O}_2 + \text{Fe}_3\text{O}_4 + \text{CTABr}$	47.89	45.27	144.484	0.962

Reaction conditions: pH = 3.0, Fe_3O_4 = 0.1% w/v, [CTABr] = $2.0 \times 10^{-2} \text{ mol dm}^{-3}$

Conclusions

The studies on the oxidation of MB in the presence of Fe_3O_4 nanoparticles enhances the rate of oxidation by H_2O_2 . The Fe_3O_4 nanoparticles were synthesized by the co-precipitation method and was characterized by using the physicochemical techniques like XRD, VSM, SEM, TEM, and FT-IR. The XRD studies confirmed the crystalline nature of the synthesized material. The magnetic property was ascertained by VSM studies. The particle size, agglomeration behaviour and their shape were determined by SEM and TEM studies. The presence of Fe_3O_4 nanoparticles enhanced the rate of degradation of MB by H_2O_2 . The rate of oxidation of MB increased with the increase in the amount of Fe_3O_4 nanoparticles. The pH at which the maximum rate of degradation of MB observed was 3. The rate of reaction increased with the increase in [H_2O_2] in the absence of Fe_3O_4 nanoparticle, whereas, in the presence of Fe_3O_4 , the rate constant versus [H_2O_2] gave peaked behaviour. In the presence of surfactant, CTABr increased the rate of oxidation of MB by the H_2O_2 . The kinetics and the mechanistic studies can be the useful technique for the effective removal of methylene blue from the waste water at room temperature with the views of green prospective and low cost.

Acknowledgments

The authors thank UGC, New Delhi for providing financial assistance in the form of scholarship and contingency.

Keywords

Fe_3O_4 magnetic nanoparticles, co-precipitation method, methylene blue, degradation, waste water treatment.

Received: 20 July 2020

Revised: 11 September 2020

Accepted: 22 September 2020

References

- Dalali, N.; M. Khoramnezhad, M.; Habibizadeh, M.; Faraji, M. Magnetic Removal of Acidic Dyes from Waste Waters Using Surfactant - Coated Magnetite Nanoparticles: Optimization of Process by Taguchi Method, Int. Conf. Environ. Agric. Eng. IPCBEE, **2011**, 15, pp.89-93.
- Mahmoudi, Z.; Azizian, S.; Lorestani, B.; *J. Mater. Environ. Sci.*, **2014**, 5, 1332.
- Youssef, N.A.; Shaban, S.A.; Ibrahim, F.A.; Mahmoud, A.S.; *Egypt. J. Pet.*, **2016**, 25, 317.
- Zhou, Y.; Yanbo, L.; Zhou, Y.; Liu, Y.; *Environ. Pollut.*, **2019**, 252, 352.
- Cao, Z.; Fang, W.X.; Chen, P.; Yang, F.; Ou, X.; Li, W.S.; Zhong, H.; *Coll. Surf. A: Physicochem. Eng. Asp.*, **2018**, 549, 94.
- Jiaqi, Z.; Yimin, D.; Danyang, L.; Shengyun, W.; Liling, Z.; Yi, Z.; *Coll. Surf. A: Physicochem. Eng. Asp.*, **2019**, 572, 58.

7. Foroutan, R.; Mohammadi, R.; Razeghi, J.; Ramavandi, B.; *Algal Res.*, **2019**, *40*, 101509.
8. Sun, C.; Yang, S.T.; Gao, Z.; Yang, S.; Yilihamu, A.; Ma, Q.; Zhao, R.S.; Xue, F.; *Mater. Chem. Phys.*, **2019**, *223*, 751.
9. Zhang, Q.; Yu, L.; Xu, C.; Zhao, J.; Pan, H.; Chen, M.; Xu, Q.; Diao, G.; *Appl. Surf. Sci.* **2019**, *483*, 241.
10. Anjum, M.; Miandad, R.; Waqas, M.; Gehany, F.; Barakat, M.A.; *Arab. J. Chem.*, **2019**, *12*, 4897.
11. Misdan, N.; Lau, W.J.; Ong, C.S.; Ismail, A.F.; Matsuura, T.; *Korean J. Chem. Eng.* **2016**, *32*, 753.
12. Saleh, R.; Taufik, A.; *J. Environ. Chem. Eng.*, **2019**, *7*, 102895.
13. Tayade, R.J.; Natarajan, T.S.; Bajaj, H.C.; *Ind. Eng. Chem. Res.*, **2009**, *48*, 10262.
14. Rafatullah, M.; Sulaiman, O.; Hashim, R.; Ahmad, A.; *Journal of Hazardous Materials*, **2010**, *177*, 70.
15. Vakili, M.; Rafatullah, M.; Salamatinia, B.; Abdullah, A.Z.; HakimIbrahim, M.; Tan, K.B.; Gholami, Z.; Amouzgar, P.; *Carbohydrate Polymers*, **2014**, *113*, 115.
16. Akil Ahmad, A.; Mohd-Setapar, S.H.; Chuong, C.S.; Khatoon, A.; Wani, W.A.; Kumar, R.; Rafatullah, M.; *RSC Advances*, **2015**, *5*, 30801.
17. Divriklioglu, M.; Akar, S.T.; Akar, T.; *Environ. Sci. Pollut. Res.*, **2019**, *25*, 25834.
18. Kumar, A.; Sharma, G.; Naushad, M.; Singh, P.; Kalia, S.; *Ind. Eng. Chem. Res.*, **2014**, *53*, 15549.
19. Alishiri, T.; Oskooei, H.A.; Heravi, M.M.; *Synth. Commun.*, **2013**, *43*, 3357.
20. Godoi, M.; Liz, D.G.; Ricardo, E.W.; Rocha, M.S.T.; Azeredo, J.B.; Braga, A.L.; *Tetrahedron*, **2014**, *70*, 3349.
21. Kumar, A.; Gupta, M.; *Biomaterials*, **2005**, *26*, 3995.
22. Mahdavi, S.; Jalali, M.; Afkhami, A.; Removal of heavy metals from aqueous solutions using Fe₃O₄, ZnO, and CuO nanoparticles, in: *Nanotechnology for Sustainable Development*. Springer International Publishing, **2012**, pp.171-188.
23. Jaafarzadeh, N.; Takdastan, A.; Jorfi, S.; Ghanbari, F.; Ahmadi, M.; Barzegar, G.; *J. Mol. Liq.*, **2018**, *256*, 462.
24. Jiang, J.; Zou, J.; Zhu, L.; Huang, L.; Jiang, H.; Zhang, Y.; *J. Nanosci. Nanotechnol.*, **2011**, *11*, 4793.
25. Reza, K.M.; Kurny, A.; Gulshan, F.; *Int. J. Environ. Sci. Dev.*, **2016**, *7*, 325.
26. Rashad, M.M.; Ibrahim, A.A.; Rayan, D.A.; Sanad, M.M.S.; Helmy, I.M.; *Environ. Nanotechnology, Monit. Manag.*, **2017**, *8*, 175.
27. Azcona, P.; Zysler, R.; Lassalle, V.; *Colloids Surfaces A Physicochem. Eng. Asp.* **2016**, *504*, 320.
28. Li, M.Y.; Sui, X.D.; *Key Eng. Mater.*, **2012**, *512*, 82.
29. Márquez, F.; Herrera, G.M.; Campo, T.; Cotto, M.; Ducongé, J.; Sanz, J.M.; Elizalde, E.; Perales, O.; Morant, C.; *Nanoscale Res. Lett.*, **2012**, *7*, 210.
30. Raees, K.; Ansari, M.S.; Rafiquee, M.Z.A.; *J. Nanostructure Chem.*, **2019**, *9*, 175.
31. Saranya, T.; Parasuraman, K.; Anbarasu, M.; Balamurugan, K.; *Nano Vis.*, **2015**, *5*, 149.
32. Aliramaji, S.; Zamanian, A.; Sohrabijam, Z.; *Procedia Mater. Sci.*, **2015**, *11*, 265.
33. Saif, B.; Wang, C.; Chuan, D.; Shuang, S.; *J. Biomater. Nanobiotechnol.*, **2015**, *6*, 267.
34. Salem, I.A.; El-Maazawi, M.S.; *Chemosphere*, **2000**, *41*, 1173.
35. Wang, B.; Yin, J.-J.; Zhou, X.; Kurash, I.; Chai, Z.; Zhao, Y.; Feng, W.; *J. Phys. Chem. C*, **2013**, *117*, 383.
36. Lin, S. S.; Gurol, M.D.; *Environ. Sci. Technol.* **1998**, *32*, 1417.
37. Sun, J. H.; Sun, S. P.; Wang, G. L.; Qiao, L. P.; *Dye. Pigment.* **2007**, *74*, 647.
38. Sun, J. H.; Shi, S. H.; Lee, Y. F.; Sun, S. P.; *Chem. Eng. J.*, **2009**, *155*, 680.
39. Kavitha, V.; Palanivelu, K.; *Water Res.* **2005**, *39*, 3062.
40. Sun, J.; Sun, S.; Sun, J.; Sun, R.; Qiao, L.; Guo, H.; Fan, M.; *Ultrason. Sonochem.* **2007**, *14*, 761.
41. Gulkaya, I.; Surucu, G.; Dilek, F.; *J. Hazard. Mater.* **2006**, *136*, 763.
42. Khan, A.M.; Mehmood, A.; Sayed, M.; Nazar, M.F.; Ismail, B.; Khan, R.A.; Ullah, H.; Abdur Rehman, H.M.; Khan, A.Y.; Khan, A.R.; *J. Mol. Liq.*, **2017**, *236*, 395.